DOI 10.2478/ama-2025-0090

ANALYSIS OF TRANSVERSE NATURAL VIBRATION OF AVIATION TRANSMISSIONS TOOTHED WHEELS WITH USING CYCLIC SYMMETRY PROPERTIES

Stanisław NOGA*, Paweł FUDALI*

*Faculty of Mechanical Engineering and Aeronautics, Department of Mechanical Engineering, Rzeszów University of Technology, al. Powstańców Warszawy 8, 35-959 Rzeszów, Poland

noga@prz.edu.pl, pfudali@prz.edu.pl

received 29 October 2025, revised 16 December 2025, accepted 21 December 2025

Abstract: The paper discusses the issue of transverse natural vibrations of toothed wheels intended for operation in aviation power transmission systems or in the transmission of aircraft engine aggregates. The discussion was conducted using wheels with straight, oblique and circular-arc teeth, as well as with a full wheel disc and a wheel disc with eccentric holes. In the analysis process, simplified toothed ring models were proposed for each gear in the form of rings made of a hypothetical material with satisfactory physical properties (equivalent values of Young's modulus and the density). In the proposed models were also taken into account the properties of cyclic symmetry exhibited by the studied objects. The calculation process was carried out using the finite element method and the commercial ANSYS software. The influence of the type and size of finite element on the quality of the obtained results was also investigated. The main part of the work concerns the assessment of the usefulness of the proposed simplified models of the analyzed wheels in the vibration simulation process. In order to confirm the correctness of the simulation research methodology, for one of the analyzed wheel cases, the numerical simulation results were verified experimentally on a real object. The article concludes with remarks and conclusions regarding the obtained results. The issues presented in this paper may be useful in engineering practice related to vibrations of circularly symmetric systems (in particular, gear wheels).

Key words: cyclic symmetry modeling, toothed gears transverse vibration, circular plate vibration, FEM solution, simplified toothed ring model

1. INTRODUCTION

The growing of modern technology requires the creation of devices characterized by high durability and operational reliability. This applies particularly to machine components and assemblies manufactured for the aviation industry [1, 2]. Each newly designed component or assembly must undergo an appropriate set of simulation tests to be approved for further development stages related to its final application in aircraft structures. One of the important factors that may significantly disrupt or limit the functioning of aviation structure elements is the possibility for vibrations occurring of individual elements or assemblies [1, 3]. For economic reasons and the reliability of the results, it is advantageous to conduct simulation calculations using appropriate calculation procedures using dedicated commercial software [2, 3].

The rapid development of computer technology and computational systems based, among others, on the finite element method (FEM) allows for the analysis of vibrations of systems characterized by complex structure and geometry [1, 2, 4]. Publication [3] is one of the first scientific works that comprehensively discusses the issues of vibrations of gear wheels in aviation transmissions, taking into account simulation and experimental studies. In the FEM simulation models used in this work an axisymmetric approach is utilized. The books [1, 5] comprehensively discuss the issue of vibrations, taking into account the issues of vibration modeling and measurement, with the work [1] referring mainly to measurement techniques and the work [5] concerning the theory of vibrations of continuous systems, including circularly symmetric systems. In the work [2] the problem of vibrations of systems with circular symmetry (gears, rings with an elastic layer) was discussed using FEM simulation techniques and theoretical analysis. In the above work, only one case of a gear wheel was considered. The book publication [4] primarily discusses the issue of quality measures for developed FEM simulation models. This information was used, among others, in the work [6] to effectively develop a numerical FEM model of the shaft cover of an aircraft engine turbine for the purpose of vibration analysis. In paper [7] is proposed a mathematical model based on a physical neutral surface (PNS) for the natural vibrations analysis of functionally graded (FG) thin circular annular plates with a power-law distribution of material properties along the thickness and various boundary conditions. The proposed approach was numerically verified using FEM. In the paper [8] the issues of transverse vibration of gear wheel with geometric discontinuities in the form of through holes in the discs were discussed using FEM numerical methods. The discussed issues mainly concerned the proposed in the paper algorithm for determining the deformed mode shapes of transverse vibrations of the wheel. The article [9] also discusses gear vibration issues using simulation techniques similar to those in the previously mentioned work. The numerical analyses required in the mentioned paper were performed using full FEM models of discussed gear wheels.. In the works [10, 11, 12] the theoretical basis of the methodology for analyzing the vibration of systems characterized by cyclic symmetry properties was discussed.

Among other things, paper [10] presents a method for analyzing the steady-state vibrations of cyclically symmetric bladed discs subjected to arbitrary loads distributed in space and periodic in time. The authors of [11] used the dynamic properties of cyclically symmetric structures to develop a method for detecting damage in the form of gaps and cracks. The proposed method utilizes an analysis of the sensitivity of natural frequencies to changes in the system's design parameters. Whereas, the PhD disertation [12] investigates the modal properties of general cyclically symmetric systems and multistage systems with cyclically symmetric stages, such as planetary gears, systems with centrifugal pendulum vibration absorbers (CPVAs), multistage planetary gears, etc. Methods are proposed to improve the computational efficiency for numerically solving the vibration equations of discussed cyclically symmetric structures. In the paper [13] the transverse vibrations of a circularly symmetric plate with complex geometry were discussed using the properties of cyclic symmetry and experimental studies. Similarly, in the work [14] the problem of transverse vibrations of a circularly symmetric plates with eccentric holes was analyzed using numerical simulation and experimental tests. In the proposed finite element (FE) models of the plates the observed properties of cyclic symmetry were utilized. The cyclic symmetry model proposed in the paper [13] represented one-sixth part of the whole plate, and each cyclic symmetry model in the article [14] represented one-fifth part of the each plate analyzed. Paper [15] discusses the rules governing the splitting or non-splitting of natural frequencies for any nodal diameter for an axisymmetric annular stepped plate with circumferentially uniformly spaced groups of mass blocks. The proposed analytical solutions were verified by numerical and experimental studies. In the paper [16] there is proposed an extension of the spectro-geometric method (SGM), which is addressed to the orthotropic vibration problem of rectangular plates, to analyze the free and forced vibrations of annular sector plates and annular plates subjected to general boundary constraints (including cyclic symmetry). The effectiveness of the methodology was confirmed by numerical simulations. In the works [17, 18] simplified FEM models were effectively used to analyze the problems of transverse vibrations of gears, in which, after omitting the meshing geometry, it was possible to use the properties of cyclic symmetry. The models with cyclic symmetry proposed in the article [17] constituted one sixth part of each analyzed wheel. Whereas the simplified FE models proposed in the work [18] referred to the cases of two spur gears with straight teeth. In the papers [19, 20] the static and dynamic issues of the strength of gears with an unusual tooth profile and the problems of determining the contact pattern area in gear meshing were discussed. The effectiveness of the proposed methodology has been confirmed by numerical simulations and experimental studies. Paper [21] analyzes the in-plane flexural vibrations of a periodic electric motor stator modeled by a circular ring with cyclically symmetric properties and taking into account magnetic phenomena. The proposed methodology was numerically verified using the finite element method. Article [22] proposes a method for solving the free vibration equation of rotationally repetitive structures, enabling the optimal design of cyclically symmetric structures with frequency constraints. The effectiveness of the proposed method was numerically verified on two large-scale axisymmetric objects. Much work concerns the use of cyclic symmetry properties in modeling turbine disks (including the previously mentioned work [10]). Paper [23] demonstrates the use of cyclic symmetry properties in the vibration analysis of multistage structures, such as compressors or turbines in turbomachinery. Example results obtained using FEM are presented. In article [24], a numerical method for analyzing the vibrations of a turbine disc with blades was proposed, utilizing the cyclic symmetry properties of the structure. In the analysis process the friction phenomenon in the blade mounting area was included. In article [25] there are discussed the development a high-fidelity full-rotor aeromechanics analysis capability for a system subjected to distorted inlet flow by employing a cyclically symmetric finite element modeling approach. The numerical analysis results were validated by wind tunnel tests. The paper [26] presents a reduced-order modeling process applied to the study of vibrations of systems with circular symmetry (the stator vane model). The relevant vibration equations were solved using the harmonic balance procedure and a classical iterative nonlinear solver.

Present work discusses the transverse natural vibrations of toothed wheels intended for operation in aviation power transmission systems or in the transmission of aircraft engine aggregates. The cases of gears with straight, oblique and circular arc teeth were analyzed. In the considerations, simplified toothed rim models were proposed for each gear in the form of rings made of a hypothetical material with satisfactory physical properties (equivalent values of Young's modulus and the density). In the proposed models were also taken into account the properties of cyclic symmetry observed in the studied objects. For four discussed wheels, four simplified models with different segment angles were considered. Two models with cyclic symmetry properties were proposed for a wheel with eccentric holes. The influence of the type and size of finite element on the quality of the obtained results was also investigated. To confirm the validity of the simulation research methodology, for one of the analyzed gears, the results of the numerical simulations were experimentally verified on a real object. The above-mentioned research scope constitutes, in the authors' humble opinion, a new approach to the research topic being pursued, significantly expanding the research discussed in other works by the authors. The main part of the work is the assessment of the usefulness of the proposed simplified models of the analyzed wheels in the vibration simulation process. The article is a continuation of the authors research work relating to the issues of static and dynamic of toothed wheels.

2. FORMULATION OF THE PROBLEM

The object of consideration in this paper is the analysis of transverse vibrations of aircraft transmissions gear wheels. Such wheels are required to be highly reliable while maintaining the lowest possible weight [2, 3]. Hence the need to conduct dynamic analyzes at the design stage to assess the possibility of wheel vibrations occurring during operations [2, 3]. Due to their geometric shape and the nature of work, gear wheels are most often exposed to transverse vibrations. Modern computational methods using FEM allow for all kinds of dynamic analyzes by using numerical models of engineering objects [1, 2, 4]. Typically, numerical analyzes of dynamic problems consume significant hardware resources of computing machines. It becomes reasonable to develop a methodology that will significantly reduce the hardware needs during FEM numerical calculations, while maintaining the quality parameters of the obtained results, in the sense of the adopted criterion.

The main goal of this work is to discuss the methodology for preparing FE (finite element) models of toothed gears, taking into account the cyclic symmetry properties of the considered systems. In this approach, the geometric features of rotational structural elements are used, the shape of which can be composed of a finite number of identical segments arranged symmetrically with respect to the axis of rotation. Each such segment, apart from being

DOI 10.2478/ama-2025-0090

identical in shape and material, is subject to identical physical phenomena during the operation of the rotating element to which it belongs. Each segment has two boundary areas of cooperation with neighboring segments, called side 1 and side 2 (see Fig. 1). Physical phenomena occurring in individual segments must satisfy the compatibility conditions at the boundaries between segments, i.e. [11, 12]:

$$u_1^{n_K+1} = u_1^{n_K},\ n_K = 1,2,\dots,N \tag{1}$$

In the above equation, $u_1^{n_K+1}, u_1^{n_K}$ refer to the analyzed component of physical phenomenon in segments (displacement, force, stress, temperature, etc.), the superscript refers to the segment number, the subscript refers to the side index and *N* is the number of segments into which the system is divided. Taking into account the same physical properties of the individual segments, it can be written that $u_1^{n_K+1} = u^1$ [11]. Eq. (1) represent the constraint equation between the physical segments.

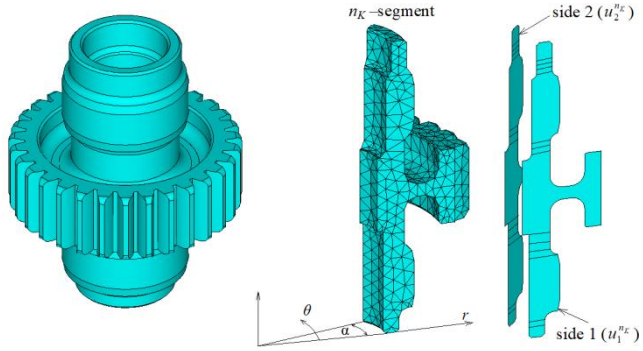

Fig. 1. Model with the n_K segment with cyclic symmetry features

The transformation equation between the physical components and the cyclic components is written in the form [11, 25]:

$$u^{n_K} = \bar{u}^0 + \sum_{k=1}^{k_L}[\bar{u}^{kc}\cos[(n_K-1)k\alpha] + \bar{u}^{ks}\sin[(n_K-1)k\alpha]] + (-1)^{n_K-1}\bar{u}^{N/2}$$

$$\alpha = 2\pi/\mathrm{N}, n_K = 1,2,\dots,N \tag{2}$$

where: u^{n_K} can be any physical component (displacement, force, etc.) in the n_Kth segment and $\bar{u}^0, \bar{u}^{kc}, \bar{u}^{ks}$ and $\bar{u}^{N/2}$ are so-called cyclic components. The summation limit k_L takes the value $k_L = (N-1)/2$ if N is odd and $k_L = (N-2)/2$ if N is even. The term α represents the angle of the segment and the term $\bar{u}^{N/2}$ exist only when N is even. The term k is the harmonic index. The Eq. 2 include the finite number of Fourier series terms so it can be called a finite Fourier transformation [12]. Using the inverse transform one can determine the cyclic components. In this work, the ANSYS software is used for analysis. In the software computational algorithms the duplicate sector method is used to solve the relevant equations which takes into acount the properties of cyclic symmetry [2, 25].

As mentioned earlier, the main objective of this paper is to discuss the methodology for creating FE models of gear wheels, with including the properties of cyclic symmetry. Taken into consideration wheels have a toothed ring with oblique (or circular-arc) or straight teeth. The design features of the analyzed wheel cases result, to a large extent, from the applications of the analyzed wheels in aviation power transmission systems or in the transmission of aircraft engine aggregates.

In the first stage, solid models of the wheels were made in CATIA software. Then, the geometry of the models was simplified by removing elements that did not significantly affect the vibration phenomenon of the systems (roundings, chamfers, etc.) [1, 2]. In the Fig. 2 it is shown the geometric models of the objects under investigation which are prepared for the next stage of the process. These are treated as the so-called basic (or reference) models of the analyzed wheels. More technical data about these wheels can be found in Tab. 1.

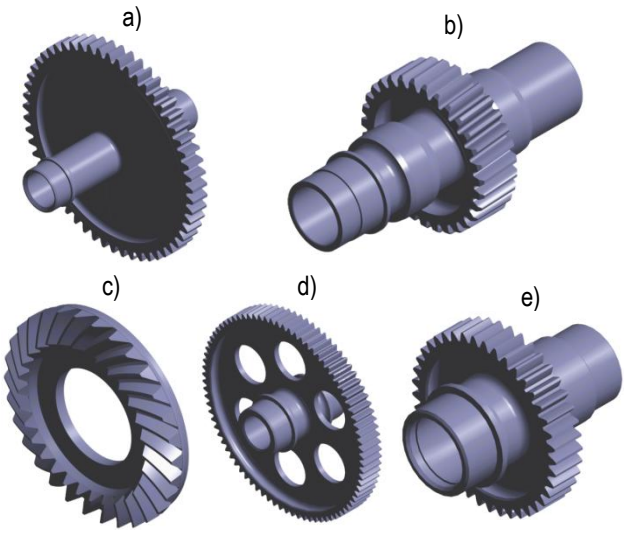

Fig. 2. Geometric models of the gears under investigation: a) GR1_1, b) GR2_1, c) GR3_1, d) GR4_1, e) GR5_1

Tab. 1. The toothed gears in question

No. of wheel	Tooth count z	Gear module m_0	Denotation in the article	Description
1	55	2.12	GR1_1	aviation toothed wheel (for aggregates, see Fig. 2a)
2	31	3	GR2_1	aviation toothed wheel (for power transmission, see Fig. 2b)
3	30	6	GR3_1	spiral bevel gear (for power transmission, see Fig. 2c)
4	83	2.5	GR4_1	aviation toothed wheel (for aggregates, see Fig. 2d)
5	41	2.5	GR5_1	aviation toothed wheel (for power transmission, see Fig. 2e)

As mentioned earlier, in the proposed simplified models the cyclic symmetry properties can be used, which can be seen by analyzing the geometry of the considered wheels. It should be expected that this method of proceeding will allow for obtaining much smaller (in terms of file size due to the complexity of the geometry) FE models and will enable a reduction in the required computational resources of computing machines. For easier identification, the full names of the individual models and their designation in the article are provided in Tab. 2.

Tab. 2. Description of the cyclic symmetry models of the discussed gears

Denotation in the article	Description	Denotation in the article	Description
GR1_2	cyclic symmetry segment model of the GR1_1 wheel, covering one tooth, cut along the centers of the inter – tooth slots ($\alpha = 6.55°$)	GR2_2	cyclic symmetry segment model of the GR2_1 wheel, covering one tooth, cut along the centers of the inter – tooth slots ($\alpha = 11.61°$))
GR1_3	cyclic symmetry segment model of the GR1_1 wheel without teeth (full ring), covering a 1/50th – circle segment ($\alpha = 7.2°$)	GR2_3	cyclic symmetry segment model of the GR2_1 wheel without teeth (full ring), covering a 1/50th – circle segment ($\alpha = 7.2°$)
GR1_4	cyclic symmetry segment model of the GR1_1 wheel without teeth (full ring), covering a 1/16th – circle segment ($\alpha = 22.5°$), see Fig. 3a)	GR2_4	cyclic symmetry segment model of the GR2_1 wheel without teeth (full ring), covering a 1/16th – circle segment ($\alpha = 22.5°$), see Fig. 3a)
GR1_5	cyclic symmetry segment model of the GR1_1 wheel without teeth (full ring), covering a 1/10th – circle segment ($\alpha = 36°$)	GR2_5	cyclic symmetry segment model of the GR2_1 wheel without teeth (full ring), covering a 1/10th – circle segment ($\alpha = 36°$)

Interesting models, in terms of their future use in systems with a complex shape of the wheel disc (e.g. holes in the disc), are simplified models in which the toothed ring is replaced by a uniform ring (see Tab. 2) with equivalent physical properties [2, 18]. In Fig. 3 it is shown examples of simplified models related to the toothed wheels in question (see Fig. 2), where toothed rings are simplified in to full rings (the yellow part of each model). In each simplified model, the outer diameter of the ring is equal the head diameter of the gear.

This approach allows to develop a simplified cyclic symmetry model of the GR4_1 wheel. For this wheel two simplified models were developed. In the first simplified model designated as GR4_3 (see Fig. 3d), the cyclic symmetry sector of the wheel GR4_1 includes the entire eccentric hole of the wheel disc. In the second simplified model of the GR4_1 wheel (model designation GR4_4, see Fig. 3e), the boundary areas of the segment are led through the centers of symmetry of the eccentric holes of the wheel disc. Both models have the same angle value $\alpha = 60°$ (angle of the segment). The description of the remaining simplified models developed is presented in Tabs. 2–3.

Tab. 3. Description of the cyclic symmetry models of the discussed gears

Denotation in the article	Description	Denotation in the article	Description
GR3_2	cyclic symmetry segment model of the GR3_1 wheel, covering one tooth, cut along the centers of the inter – tooth slots ($\alpha = 12°$)	GR4_3	cyclic symmetry segment model of the GR4_1 wheel, covering the entire eccentric hole of the wheel disc ($\alpha = 60°$, see Fig. 3d)
GR3_3	cyclic symmetry segment model of the GR3_1 wheel without teeth (full ring), covering a 1/50th – circle segment ($\alpha = 7.2°$)	GR4_4	cyclic symmetry segment model of the GR4_1 wheel where the boundary areas of the segment are led through the centers of symmetry of the eccentric holes of the wheel ($\alpha = 60°$, see Fig. 3e)
GR3_4	cyclic symmetry segment model of the GR3_1 wheel without teeth (full ring), covering a 1/16th – circle segment ($\alpha = 22.5°$, see Fig. 3a)	GR5_2	cyclic symmetry segment model of the GR5_1 wheel, covering one tooth, cut along the centers of the inter – tooth slots ($\alpha = 8.78°$)
GR3_5	cyclic symmetry segment model of the GR3_1 wheel without teeth (full ring), covering a 1/10th – circle segment ($\alpha = 36°$)	GR5_3	cyclic symmetry segment model of the GR5_1 wheel without teeth (full ring), covering a 1/50th – circle segment ($\alpha = 7.2°$)
GR5_4	cyclic symmetry segment model of the GR5_1 wheel without teeth (full ring), covering a 1/16th – circle segment ($\alpha = 22.5°$, see Fig. 3a)	GR5_5	cyclic symmetry segment model of the GR5_1 wheel without teeth (full ring), covering a 1/10th – circle segment ($\alpha = 36°$)

The problems of natural vibrations of the discussed systems were solved using the finite element method in the ANSYS computational software. The wheels in question can be treated as annular plates of a complex shape, with four of them additionally installed on hollow stepped shafts [1, 5]. For this reason, for each solution for which the nodal lines are nodal diameters, one obtain two identical systems of nodal lines, rotated with respect to each other by an angle $\beta = \pi/(2n)$, where n is the number of nodal diameters. In accordance with the circular and annular plate vibration theory, in this paper the particular natural frequencies of vibration are denoted by ω_{mn}, where m refers to the number of nodal circles and n refers to the mentioned number of nodal diameters [5].

DOI 10.2478/ama-2025-0090

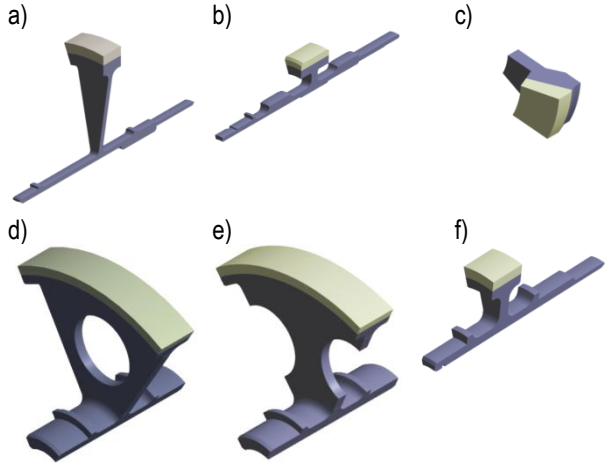

Fig. 3. Examples of simplified geometric models of the discussed gears with full ring: a) GR1_4, b) GR2_4, c) GR3_4, d) GR4_3, e) GR4_4, f) GR5_4

3. FINITE ELEMENT REPRESENTATION OF THE DISCUSSED SYSTEMS

The developed geometric models (basic/reference – see Fig. 2 and simplified – see Fig. 3 and Tabs. 2 and 3) were meshed by using available procedures of the ANSYS software. In order to test different variants and obtain general knowledge, three types of finite elements were used in the meshing process, i.e. solid185, solid186 and solid187. The Solid185 element is an eight-node brick element with three degrees of freedom at each node (nodal translations in three mutually perpendicular directions). The solid186 element is a higher-order brick element consisting of twenty nodes and three degrees of freedom at each node. The solid187 element is a ten-node higher-order tetrahedral element and, like in the previous case, has three degrees of freedom at each node. This element is well-suited and recommended for meshing systems with irregular geometry [2, 4, 25]. During the meshing process, the maximum length of each element side was assumed to be no greater than 1 [mm]. Including simplified models, fifteen FE model cases were considered for each of the GR1_1 and GR5_1 wheels, thirteen FE model cases were considered for each of the GR2_1 and GR3_1 wheels, and nine FEM model cases were considered for the GR4_1 wheel. Due to difficulties in generating a high-quality FEM mesh, the results obtained for the simplified GR2_2_m and GR3_2_m models with solid185 and solid186 elements were not considered.

Tab. 4. Description of the FE models of the discussed gears

Model	Type of element	No. of nodes	No. of elements
GR1_1_m	solid185	67248	48690
	solid186	252018	48690
	solid187	302701	175996
GR1_2_m	solid185	986	474
	solid186	10684	1740
	solid187	7937	3912
GR1_3_m	solid185	4415	2756
	solid186	15592	2756
	solid187	26348	15784
GR1_4_m	solid185	12544	9295
	solid186	46017	9295
	solid187	61715	39127
GR1_5_m	solid185	19867	11476
	solid186	57726	11476
	solid187	35246	19867
GR2_1_m	solid185	301199	274231
	solid186	1159443	269157
	solid187	1864765	1255089
GR2_2_m	solid187	24814	13141
GR2_3_m	solid185	10040	6988
	solid186	36823	6984
	solid187	19767	10445
GR2_4_m	solid185	27958	22633
	solid186	105797	22529
	solid187	50490	29057
GR2_5_m	solid185	42042	34980
	solid186	159088	34500
	solid187	75913	44480

Information on the number of elements and nodes in the developed FEM models is provided in Tabs. 4 and 5. Selected FEM reference models (full model) of the analyzed wheels are shown in Fig. 4. While in Fig. 5 it is shown examples of simplified models (taking into account the properties of cyclic symmetry) of the wheels in question.

Tab. 5. Description of the FE models of the discussed gears

Model	Type of element	No. of nodes	No. of elements
GR3_1_m	solid185	589498	517008
	solid186	2282912	517008
	solid187	1982857	1311702
GR3_2_m	solid187	88522	57266
GR3_3_m	solid185	13981	11516
	solid186	53317	11516
	solid187	19617	10780
GR3_4_m	solid185	40871	35796
	solid186	158222	35796
	solid187	54010	30838
GR3_5_m	solid185	64379	57024
	solid186	249935	57024
	solid187	83817	48093
GR4_1_m	solid185	531889	459614
	solid186	2050232	459210

	solid187	2344962	1551003
GR4_3_m	solid185	91201	78860
	solid186	352131	78860
	solid187	152873	93255
GR4_4_m	solid185	92403	80593
	solid186	359510	80593
	solid187	156865	96142
GR5_1_m	solid185	211681	194979
	solid186	827639	194979
	solid187	513791	301014
GR5_2_m	solid185	7002	4925
	solid186	26853	4925
	solid187	33275	20285
GR5_3_m	solid185	7296	5215
	solid186	27022	5215
	solid187	15102	8055
GR5_4_m	solid185	19472	15615
	solid186	72705	15615
	solid187	37489	21520
GR5_5_m	solid185	30250	24816
	solid186	114078	24816
	solid187	58919	34468

In the developed FE models there are two types of boundary conditions. The first type of boundary conditions refers to cyclic symmetry properties and is imposed systemically (through appropriate software procedures) after defining such properties. These types of boundary conditions only appear in simplified FE models of the wheels discussed. It is important in this case to use the same mesh layout (the same division into finite elements) on the boundary areas in each sector [2, 25]. Another kind of boundary condition results from the mounting or bearing method of the wheels in question. In this case, in all FE models (basic and simplified) of the wheels, the appropriate degrees of freedom were removed on the surfaces interacting with the bearings.

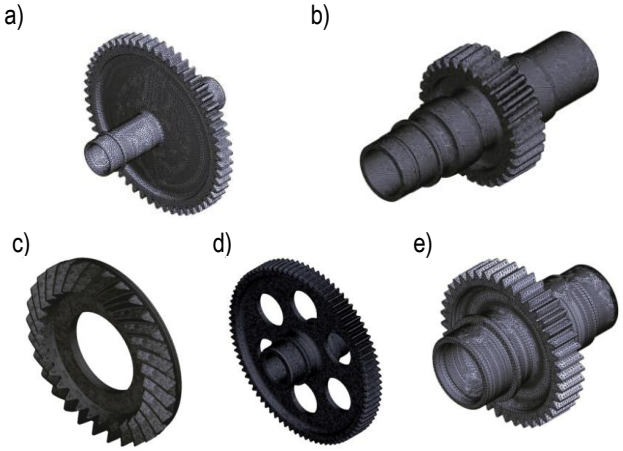

Fig. 4. FEM models (reference FEM models) of the gears under investigation: a) GR1_1_m, b) GR2_1_m, c) GR3_1_m, d) GR4_1_m, e) GR5_1_m

The quality of the proposed FEM models is determined by calculating the relative frequency error (the so-called frequency error), defined by the following Eq. [2,4]:

$$\varepsilon = (\omega^f - \omega^e)/\omega^e \times 100\% \quad (3)$$

where ω^f is the natural frequency comes from the numerical model and ω^e is the natural frequency of the reference system.

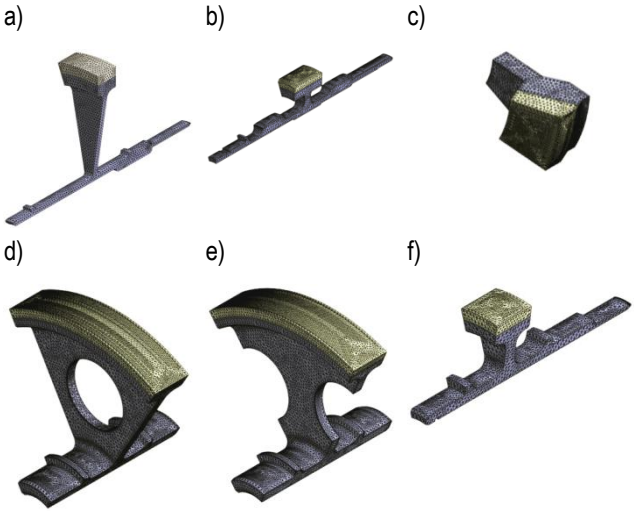

Fig. 5. Examples of simplified FE models of the discussed gears with full ring: a) GR1_4_m, b) GR2_4_m, c) GR3_4_m, d) GR4_3_m, e) GR4_4_m, f) GR5_4_m

4. NUMERICAL ANALYSIS

Based on all the previously discussed FEM models, numerical calculations were performed to determine the natural frequencies and their corresponding transverse vibration modes. The analyzed systems are made of steel with physical properties given in Table 6.

Tab. 6. Technical data related to the discussed models

No. of wheel	Young modulus E [Pa]	Density ρ [kg/m3]	Poisson's ratio ν	Equivalent Young's modulus E_z [Pa]	Equivalent density ρ_z [kg/m3]
1	$2.03 \cdot 10^{11}$	$7.86 \cdot 10^3$	0.3	$2.9 \cdot 10^9$	$4.0583 \cdot 10^3$
2					$4.3568 \cdot 10^3$
3					$3.8928 \cdot 10^3$
4					$4.0387 \cdot 10^3$
5					$3.9492 \cdot 10^3$

As mentioned earlier, in order to obtain similar physical properties of models with omitted tooth geometry (with full ring, see Tables 2 and 3) to those of the relevant reference models, it was necessary to determine equivalent values of the Young's modulus E_z and the density ρ_z of the tooth modeling rings. The geometrical dimensions of the simplified models were assumed to be the same as those of the modeled wheels. In each simplified model it was assumed that the outer diameter of the rim modelling the gear ring is equal to the head diameter of the corresponding gear wheel. With the exception of Young's modulus and the density of the rim, the same technical data was assumed for the simplified models as for the corresponding gears. In each simplified model, the density parameter of the rim was determined based on the volume fraction of the modeled

gear ring in that rim. Young's modulus of the rim of the each simplified model is selected during numerical simulation to be in accordance with the reference solution in terms of the adopted criterion (3). The numerical simulation results presented in this paper were obtained with the values of the substitute quantities mentioned, relating to individual wheels, given in Tab. 6. For all model cases, calculations were performed over a wide frequency range until the frequency value ω_{16} was determined.

At the beginning, statistical data will be discussed. The following statistical parameters were taken into account: WO – relative elapsed time, MU – sum of memory used by all processes [GB], RU – sum of disk space used by all processes [GB]. The WO parameter determines the relative computational time related to

the numerical analysis time of the reference FE models of discussed wheels. For this reason, WO = 1 was assumed for each reference FE model of the wheels in question (see Tabs. 7-10). If for a given simplified model WO < 1 it means that the calculation time of this model is shorter than the calculation time of the basic model, in the case when WO > 1 the calculation time is longer. The statistical data presented below were obtained using a computer with the following technical parameters in the calculation process: processor CPU – 4 Cores, Threads @3.8GHz, Cache 6MB, RAM memory – 4 x 8GB, DDR4 SDRAM, software ANSYS Workbench 2025 R1. In Tabs. 7-10 there are presented the statistical data recorded during the dynamic analyses of the reference and simplified FE models discussed.

When analyzing the data from Tab. 7, it is noted that for all FE models of the GR1_1 wheel , in terms of all parameters, the most favorable results (the lowest values) were obtained using the solid185 element, and the relatively worst results were obtained using the solid186 element.

In the case of the GR2_1 wheel (see Tab. 8), for all models the most favorable values of the WO parameter were recorded using the solid187 element and the weakest for the case of the solid185 element. The MU and RU parameters have the most favorable values for the solid185 element. When analyzing only simplified models, the weakest results are obtained for the case of the solid186 element. It should also be noted that in the case of the simplified model GR2_2_m, it was not possible to develop FE models with solid185 and solid186 elements of sufficient quality.

Tab. 7. Calculation statistics data for FE models of the GR_1_1 wheel

Model	WO			MU			RU		
	solid185	solid186	solid187	solid185	solid186	solid187	solid185	solid186	solid187
GR1_1_m	1	1	1	2.57	15.51	10.98	0.5	2.2	2.26
GR1_2_m	0.16	0.58	0.32	0.06	0.86	0.47	0.03	0.38	0.21
GR1_3_m	0.65	0.88	1.72	0.25	1.39	2.23	0.1	0.9	1.12
GR1_4_m	0.68	1.39	1.88	0.88	5.32	6.49	0.42	1.82	2.23
GR1_5_m	0.61	1.05	0.41	1.14	6.92	2.66	0.61	3.21	1.98

Tab. 8. Calculation statistics data for FE models of the GR_2_1 wheel

Model	WO			MU			RU		
	solid185	solid186	solid187	solid185	solid186	solid187	solid185	solid186	solid187
GR2_1_m	1	1	1	14.39	31.4	40.61	3.49	21.1	27.8
GR2_2_m	-	-	0.03	-	-	6.50	-	-	5.36
GR2_3_m	0.94	0.15	0.05	2.52	14.18	5.22	3.11	11.94	6.15
GR2_4_m	1.13	0.21	0.05	8.60	29.66	15.57	3.95	14.98	7.17
GR2_5_m	1.06	0.19	0.04	13.49	25.99	14.53	4.77	11.80	7.47

Tab. 9. Calculation statistics data for FE models of the GR_3_1 wheel

Model	WO			MU			RU		
	solid185	solid186	solid187	solid185	solid186	solid187	solid185	solid186	solid187
GR3_1_m	1	1	1	27.56	36.93	32.39	6.22	23.46	22.08
GR3_2_m	-	-	0.41	-	-	24.17	-	-	11.69
GR3_3_m	0.17	0.49	0.058	4.61	31.74	6.11	2.33	12.31	3.29
GR3_4_m	0.17	1.43	0.055	14.09	14.53	15.16	3.29	14.46	4.31
GR3_5_m	0.39	6.67	0.18	29.77	29.83	32.53	4.54	9.99	8.97

Tab. 10. Calculation statistics data for FE models of the GR_4_1 and GR5_1 wheels

Model	WO			MU			RU		
	solid185	solid186	solid187	solid185	solid186	solid187	solid185	solid186	solid187
GR4_1_m	1	1	1	24.62	48.40	41.78	6.90	31.94	36.65
GR4_3_m	1.14	1.29	0.07	26.14	29.25	15.46	8.32	25.77	7.86
GR4_4_m	1.41	1.45	0.07	26.98	29.85	15.74	8.44	23.89	7.94
GR5_1_m	1	1	1	8.61	24.16	13.18	1.77	14.40	10.41
GR5_2_m	0.44	0.05	0.01	1.43	9.21	8.96	0.99	4.17	2.69
GR5_3_m	0.79	0.06	0.01	1.47	9.46	3.39	1.22	4.89	2.53
GR5_4_m	1.10	0.10	0.02	5.03	18.54	9.84	1.57	5.73	3.05
GR5_5_m	1.26	0.15	0.02	8.61	32.63	16.80	2.01	8.95	3.94

In the case of the GR3_1 wheel models (see Tab. 9), the WO parameter is most favorable for the solid187 element, and the remaining parameters (MU and RU) are most favorable for the solid185 element and least favorable for the solid186 element. As before, no simplified FEM GR3_2_m models with solid185 and solid186 elements were developed with satisfactory quality.

Similarly, in the case of the GR4_1 and GR5_1 wheel models (see Tab. 10), the WO parameter is the most favorable for the solid187 element. For simplified models of the GR1_1 wheel, for the MU and RU parameters, the best values are observed for the solid187 element and the weakest for the solid186 element. In the case of simplified FE models of the GR51_1 wheel, the most favorable values of the MU and RU parameters are observed for the solid185 element and the weakest for the solid 186 element.

Considering the observed statistical results (relative elapsed time (WO parameter) and computer resource consumption (MU and RU parameters)) and the ease of generating simplified models of satisfactory quality, it seems reasonable to conclude that it is beneficial to use the solid187 element in the FEM mesh generation process of individual models. As mentioned earlier, it is a 3D ten-node tetrahedral element. It is also worth noting that this element is the most frequently recommended element for the implementation of calculation processes of engineering structures.

Next, issues related to the quality of the proposed simplified FE models will be discussed. In the tables below in this chapter are provided the values of the natural frequencies of the transversal vibrations of the wheels in question and the frequency errors. Taking into account the results of statistical tests, full FE models with the solid187 element were adopted as the reference models for individual wheels. The frequency values given in Tabs. 11-15 of this paper were obtained from full FE models of individual wheels with a finite element of the solid187 type. Due to the large amount of data, the values of natural frequencies for the remaining analyzed model cases are not included in this paper.

Tab. 11. Values of natural frequencies ω_{mn}[Hz] (reference FE model of the GR1_1 wheel)

		n						
		0	1	2	3	4	5	6
m	1	1613	637	1676	4584	8549	13313	18668
	2	6570	7312	8615	11307	14970		
	3	12433	14468	17164				
	4	15004						

In the case of the GR1_1 wheel (see Tab. 11), sixteen natural frequencies of transversal vibration were identified within the analyzed frequency range.

Tab. 12. Values of natural frequencies ω_{mn}[Hz] (reference FE model of the GR2_1 wheel)

		n						
		0	1	2	3	4	5	6
m	1	6615.3	4794	5630.9	11975	19232	26465	32030
	2	20610	21263	25065				

For the GR2_1 wheel (see Tab. 12), ten natural frequencies were identified within the analyzed frequency range.

Tab. 13. Values of natural frequencies ω_{mn}[Hz] (reference FE model of the GR3_1 wheel)

		n						
		0	1	2	3	4	5	6
m	1	3220	780	1471	3876.9	6905.9	10366	13986
	2	-	4901.1	8386.7	12587			

For the GR3_1 wheel (see Tab. 13), ten natural frequencies were also identified within the analyzed frequency range.

Tab. 14. Values of natural frequencies ω_{mn}[Hz] (reference FE model of the GR4_1 wheel)

		n						
		0	1	2	3	4	5	6
m	1	613	430	955	2639	4944	7796	10859
	2	4700	4944	5678	6250	9370	10267	
	3	10510						

In the case of the GR4_1 wheel (see Tab. 14), fourteen natural frequencies of transversal vibration were identified within the analyzed frequency range.

The fewest natural frequencies, i.e. nine (see Tab. 15), were identified for the case of the GR5_1 wheel.

Tab. 15. Values of natural frequencies ω_{mn}[Hz] (reference FE model of the GR5_1 wheel)

		n						
		0	**1**	**2**	**3**	**4**	**5**	**6**
m	**1**	5169	4363	4981	9836	16467	23702	31072
	2	22007	22655					

Tables 16-21 present the results relating to the quality of the discussed FE models of wheels, defined in accordance with Eq. (3) (the so-called frequency error). As mentioned earlier, the results of numerical simulations of the relevant full FE models of the wheels (i.e. GR1_1_m, GR2_1_m, GR3_1_m, GR4_1_m, GR5_1_m) with the solid187 element were used as reference data.

The results presented in Table 16 refer to the errors (frequency errors) of fitting the results obtained from the full FE models of the discussed wheels with solid185 and solid186 elements with the relevant reference data. In each analyzed case, the best fit is observed for models with a solid186 element.

The results in Tab. 17 refer to fitting errors of the frequency obtained from the simplified FEM models of the GR1_1 wheel. The best fit is obtained by results come from the GR1_2_m model with the solid187 element. In the case of the GR1_3_m model, the fit of the results come from the models with solid186 and solid187 elements is comparable. All results come from the GR1_4_m and GR1_5_m models show comparable fit to reference data.

Tab. 16. Values of the frequency error ε_{mn} [%] (comparison results comes from full FE models of wheels)

ε_{mn}	GR1_1_m		GR2_1_m		GR3_1_m		GR4_1_m		GR5_1_m	
	solid185	**solid186**	**solid185**	**solid186**	**solid185**	**solid186**	**solid185**	**solid186**	**solid185**	**solid186**
ε_{11}	-0.79	0,16	-0.61	0.02	-1.03	-0.26	-1.16	-093	0.62	-0.14
ε_{10}	-0.56	0,12	-0.70	0.02	-2.48	-0.31	-0.51	-0.02	0.57	-0.13
ε_{12}	-1,19	0,24	-1.33	0.01	-1.43	-0.14	-0.94	0.00	0.74	-0.21
ε_{13}	-1,11	0,22	-1.74	0.01	-1.14	-0.01	-1.04	0.02	0.73	-0.23
ε_{20}	-0,85	0,18	-1.60	0.01	-	-	-0.50	0.01	0.59	-0.20
ε_{21}	-1,18	0,21	-0.59	0.02	-0.49	-0.03	-0.56	0.02	0.60	-0.17
ε_{14}	-1,37	0,20	-1.97	0.01	-1.22	-0.06	-1.03	0.03	0.76	-0.25
ε_{22}	-1,50	0,24	-0.86	0.02	-0.53	-0.01	-0.67	0.01	0.62	-0.21
ε_{23}	-1,53	0,22	-1.01	0.02	-0.99	-0.08	-0.67	0.02	-	-
ε_{30}	-0,63	0,12	-	-	-	-	-0.53	0.01	-	-
ε_{15}	-1,62	0,21	-1.18	0.02	-1.40	-0.11	-1.08	0.02	0.82	-0.27
ε_{31}	-2,92	-1,24	-	-	-	-	-	-	-	-
ε_{24}	-1,59	0,19	-	-	-	-	-	-	-	-
ε_{25}	-	-	-	-	-	-	-0.81	0.01	-	-
ε_{40}	-1,16	0,20	-	-	-	-	-	-	-	-
ε_{32}	-1,43	0,23	-	-	-	-	-	-	-	-
ε_{16}	-1,91	0,21	-1.40	0.02	-084	-0.08	-1.09	-0.58	0.89	-0.29

Tab. 17. Values of the frequency error ε_{mn} [%] (comparison results comes from simplified FE models of GR1_1 wheel)

ε_{mn}	GR1_2_m			GR1_3_m			GR1_4_m			GR1_5_m		
	solid185	**solid186**	**solid187**	**solid185**	**solid186**	**solid187**	**solid185**	**solid186**	**solid187**	**solid185**	**solid186**	**solid187**
ε11	-4.08	0.16	0.00	-0.31	0.47	0.47	-0.16	0.31	0.31	-0.31	0.47	0.31
ε10	-1.74	0.25	0.06	-0.56	-0.25	-0.25	-0.56	-0.25	-0.25	-0.62	-0.25	-0.31
ε12	-1.37	0.96	0.72	-1.79	-1.43	-1.49	-1.73	-1.43	-1.43	-1.85	-1.49	-1.55
ε13	-1.00	0.94	0.74	-1.66	-1.37	-1.40	-1.59	-1.33	-1.33	-1.68	-1.40	-1.42
ε20	-1.99	0.56	0.26	-0.02	0.44	0.44	0.06	0.47	0.46	-0.05	0.44	0.37
ε14	-1.19	0.96	0.75	-1.56	-1.24	-1.24	-1.49	-1.19	-1.19	-1.59	-1.24	-1.25
ε22	-3.53	0.17	0.07	-0.98	-0.16	-0.19	-0.86	-0.15	-0.17	-1.02	-0.17	-0.33
ε23	-3.00	0.34	0.25	-0.73	0.04	0.02	-0.63	0.05	0.03	-0.77	0.03	-0.12
ε30	0.39	1.43	1.27	1.30	1.66	1.71	1.27	1.66	1.71	1.28	1.71	1.56
ε15	-1.54	1.00	0.77	-1.48	-1.07	-1.08	-1.41	-1.02	-1.03	-1.53	-1.07	-1.10

ε24	-2.49	0.30	0.21	-0.66	0.05	0.03	-0.59	0.06	0.04	-0.70	0.05	-0.11
ε40	-1.66	1.29	1.05	1.44	1.75	1.76	1.49	1.76	3.56	1.43	1.77	1.69
ε16	-1.98	1.02	0.80	-1.41	-0.90	-0.90	-1.32	-0.85	-0.85	-1.47	-0.90	-0.92

Tab. 18. Values of the frequency error ε_{mn} [%] (comparison results comes from simplified FE models of GR2_1 wheel)

ε_{mn}	GR2_2_m	GR2_3_m			GR2_4_m			GR2_5_m		
	solid187	solid185	solid186	solid187	solid185	solid186	solid187	solid185	solid186	solid187
ε_{11}	0.13	0.53	0.46	0.48	0.54	0.45	0.49	0.54	0.46	0.49
ε_{12}	-0.24	-2.33	-2.88	-2.85	-2.32	-2.87	-2.59	-2.33	-2.87	-2.59
ε_{10}	-0.20	0.31	0.25	0.26	0.32	0.23	0.28	0.31	0.23	0.28
ε_{13}	0.44	-3.13	-3.48	-3.47	-3.12	-3.49	-3.29	-3.12	-3.47	-3.29
ε_{14}	-0.63	-3.77	-4.07	-4.06	-3.76	-4.07	-3.99	-3.76	-4.07	-3.99
ε_{20}	0.32	2.43	2.43	2.41	2.43	2.42	2.42	2.43	2.42	2.41
ε_{21}	-0.19	-0.04	-0.04	-0.06	-0.04	-0.04	-0.05	-0.03	-0.04	-0.05
ε_{22}	-0.45	-1.25	-1.62	-1.61	-1.25	-1.61	-1.46	-1.25	-1.62	-1.47
ε_{15}	0.25	-3.80	-4.04	-4.06	-3.79	-4.03	4.01	-3.79	-4.03	-4.01
ε_{23}	-0.54	-2.64	-2.83	-2.82	-2.63	-2.82	-2.68	-2.64	-2.83	-2.68
ε_{16}	-0.22	-4.11	-4.34	-4.31	-4.11	-4.33	-4.23	-4.11	-4.34	-4.24

Tab. 19. Values of the frequency error ε_{mn} [%] (comparison results comes from simplified FE models of GR3_1 wheel)

ε_{mn}	GR3_2_m	GR3_3_m			GR3_4_m			GR3_5_m		
	solid187	solid185	solid186	solid187	solid185	solid186	solid187	solid185	solid186	solid187
ε_{11}	0.90	-3.08	-2.95	-3.08	-2.56	-3.08	-3.21	-2.56	-3.08	-3.08
ε_{12}	-0.36	4.46	4.49	4.46	4.83	4.62	4.49	4.76	4.28	3.54
ε_{10}	-0.37	4.66	4.69	4.66	4.10	4.01	3.85	4.10	4.04	4.01
ε_{13}	-0.36	4.35	4.35	4.35	4.00	3.82	3.74	3.97	3.85	3.85
ε_{21}	-0.37	0.35	0.36	0.35	0.83	0.73	0.63	0.79	0.77	0.75
ε_{14}	-0.36	3.90	3.91	3.90	4.03	4.03	4.01	4.03	4.03	4.03
ε_{22}	-0.32	-1.51	-1.47	-1.51	-1.15	-1.28	-1.37	-1.18	-1.27	-1.25
ε_{15}	-0.68	3.17	3.19	3.17	3.61	3.34	3.30	3.63	3.36	3.35
ε_{23}	-0.39	-1.57	-1.55	-1.57	-1.01	-1.34	-1.39	-1.00	-1.33	-1.37
ε_{16}	-0.34	3.31	3.32	3.31	3.75	3.62	3.60	3.76	3.63	3.61

In the case of the GR2_1 wheel (see Tab. 18), the best fit to the reference data is shown by the results from the simplified GR2_2_m model. The results from the remaining cases of simplified models show a slightly weaker and mutually comparable fit.

The results of fitting the simplified FE models of the GR3_1 wheel (see Tab. 19) to the reference data show significant similarity to the results for the GR2_1 wheel. The best fit to the reference data is shown by the results from the simplified GR3_2_m model and the results from the remaining cases of simplified models show a slightly weaker and mutually comparable fit.

In case of GR4_1 wheel (see Tab. 20), all results come from the GR4_3_m and GR4_4_m models show comparable fit to reference data but the results from the FE models with solid186 and solid187 elements show a slightly better fit in comparison to results from models with solid185 element.

Analyzing the results presented in Tab. 21, it is noted that the best fit to the reference data is for the GR5_2_m model, with a particular preference for the model with the solid187 element. In the remaining cases of simplified models, the fit of the results to the reference data is slightly worse and mutually comparable, but satisfactory.

Summarizing the presented results, it can be noted that in all cases of the FE models, the frequency error values are below 5%, which is satisfactory. The smallest frequency errors are observed for the FE models of GR1_1 and GR5_1 wheels (frequency error below 5%). The models that perform the worst are the simplified models of GR3_1 and Gr4_1 wheels (frequency error below 5%). For all the wheels discussed, the fit of the results obtained from simplified FE models with the solid187 element is relatively favorable.

DOI 10.2478/ama-2025-0090

Tab. 20. Values of the frequency error ε_{mn} [%] (comparison results comes from simplified FE models of GR4_1 wheel

ε_{mn}	GR4_3_m			GR4_4_m		
	solid185	solid186	solid187	solid185	solid186	solid187
ε_{11}	-3.26	-3.26	-3.26	-3.26	-3.26	-3.24
ε_{10}	-4.42	-4.26	-4.26	-4.47	-4.24	-4.26
ε_{12}	-4.21	-4.31	-4.10	-4.48	-4.33	-4.21
ε_{13}	-3.85	-3.82	-3.79	-3.89	-3.83	-3.81
ε_{20}	-1.35	-1.16	-1.18	-1.38	-1.17	-1.20
ε_{21}	-2.36	-2.14	-2.18	-2.38	-2.14	-2.17
ε_{22}	-3.44	-3.35	-3.32	-3.48	-3.37	-3.32
ε_{23}	-0.93	-0.78	-0.77	-0.90	-0.77	-0.77
ε_{15}	-3.86	-3.77	-3.68	-3.82	-3.66	-3.78
ε_{25}	-2.84	-2.59	-2.58	-2.82	-2.56	-2.56
ε_{30}	-1.89	-1.56	-1.63	-1.94	-1.52	-1.63
ε_{16}	-3.28	-3.49	-3.51	-3.21	-3.45	-3.48

Tab. 21. Values of the frequency error ε_{mn} [%] (comparison results comes from simplified FE models of GR5_1 wheel

ε_{mn}	GR5_2_m			GR5_3_m			GR5_4_m			GR5_5_m		
	solid185	solid186	solid187	solid185	solid186	solid187	solid185	solid186	solid187	solid185	solid186	solid187
ε_{11}	0.48	-0.14	-0.13	-0.69	-1.22	-1.16	-0.69	-1.21	-1.12	-0.69	-1.20	-1.12
ε_{12}	0.37	-0.40	-0.38	0.86	0.43	0.48	0.86	0.43	0.51	0.86	0.44	0.51
ε_{10}	0.33	-0.22	-0.21	-0.34	-0.76	-0.72	-0.35	-0.76	-0.70	-0.35	-0.75	-0.70
ε_{13}	0.22	-0.57	-0.56	1.76	1.52	1.54	1.76	1.52	1.55	1.76	1.53	1.55
ε_{14}	0.30	-0.58	-0.56	1.69	1.46	1.47	1.69	1.46	1.48	1.69	1.46	1.48
ε_{20}	0.33	-0.24	-0.23	-1.07	-1.57	-1.51	-1.11	-1.57	-1.45	-1.08	-1.56	-1.45
ε_{21}	0.32	-0.26	-0.24	-0.46	-0.93	-0.86	-0.48	-0.93	-0.81	-0.45	-0.92	-0.80
ε_{15}	0.43	-0.57	-0.55	1.54	1.27	1.29	1.54	1.27	1.29	1.54	1.28	1.30
ε_{22}	0.29	-0.36	-0.33	0.50	0.01	0.09	0.49	0.01	0.16	0.51	0.02	0.17
ε_{16}	0.5	-0.57	-0.55	1.44	1.12	1.14	1.45	1.12	1.15	-	-	-

5. EXPERIMENTAL INVESTIGATIONS

This section discusses the experimental research to verify the proposed FE models for the system. The Polytec measuring system (see Fig. 6) composed of PSV-400 laser vibrometer, LMS SCADAS SYSTEM and TIRAvib electrodynamic shacker, is used in the experiment. The measuring experiment is planned and performed in such a way as to identify the transverse natural forms in the system under consideration. The experiment was performed for one of the wheels discussed. Due to the technical parameters of the available measuring equipment, the GR1_1 wheel was used in the experiment. The quality of full FE models of the wheel was verified, which were generated using three types of finite element (solid185, solid186, solid187). This object was excited by harmonic signals with a wide frequency band. A grid of measurement points was superimposed on the wheel. The number of selected measurement points was 500. At each point the response of the system in the transverse direction was measured using a laser vibrometer.

The values of the excited and identified natural frequencies of the transversal vibrations of the wheel in question are given in Tab. 22. These values were treated as reference data.

Fig. 6. The laboratory test stand

Tab. 22. Experimental values of natural frequencies ω_{mn}[Hz] (the GR1_1 wheel)

ω_{mn}	ω_{11}	ω_{21}	ω_{22}	ω_{23}	ω_{24}	ω_{31}	ω_{32}
GR1_1	684.38	7460	8760	11440	15020	15390	17600

The natural frequency values obtained from the FEM analysis of the complete wheel models were compared with the experimental results presented in Table 22. Table 23 presents the frequency error values (3) resulting from the comparison of FEM results with experimental results.

Tab. 23. Values of the frequency error ε_{mn} [%] (the comparison results come from the experimental data of the GR1_1 wheel)

ε_{mn}		ε_{11}	ε_{21}	ε_{22}	ε_{23}	ε_{24}	ε_{31}	ε_{32}
GR1_1_m	solid185	-6.19	-0.83	-0.19	0.35	1.25	-3.24	-1.08
	solid186	-7.07	-2.19	-1.90	-1.38	-0.52	-4.82	-2.70
	solid187	-6.92	-1.98	-1.66	-1.16	-0.33	-5.99	-2.48

Analyzing the obtained results, it was noted that in all FE models, the largest frequency error occurs at frequencies ω_{11} (error below 7.08%) and ω_{31} (error below 6%). In the remaining frequency cases, for the model with the solid186 element, the frequency error is less than 2.71%, and for the model with the solid187 element, the frequency error is less than 2.5% and in some cases of the FE models even less than 1%.

Considering the results obtained, it can be concluded that the results obtained from each model are generally satisfactory. Nevertheless, the best fit in terms of the adopted criterion is characterised by the model with the solid185 element. The model with the solid187 element also shows comparable compliance. Considering the signs of the data in Table 23, it can be concluded that the developed FE models (except for the two natural frequencies of the FE model with the solid185 element) exhibit slightly lower stiffness compared to the actual object.

Then, the effect of mesh density on the FEM solution results is considered. Simulation studies were conducted using the full FE model of the GR_1_1 wheel. The cases with solid185, solid186 and solid187 elements were analyzed, assuming that the lengths of the finite element mesh sides did not exceed the values of 0.5 [mm], 0.7 [mm], 1 [mm], 1.5 [mm], 2 [mm], 4 [mm] and 8 [mm], respectively. In order to obtain the best possible fit with the experimental results, a model updating procedure of the FE models used was carried out. In subsequent simulation steps, the parameter relating to the density of the material from which the toothed wheel was made was varied. The results presented in this article (Tabs. 24-27) were obtained with a density coefficient of $\rho = 7758$ [kg/m^3]. For the FE models with the solid187 element, the values of the natural frequencies of the transverse vibration (see Tab. 24) and the frequency error (see Tab. 25) determined according to equation (3) are provided. For the remaining FE model cases (with the solid186 and solid185 elements), only the frequency errors are provided (see Tabs. 26-27).

Analyzing the frequency values for individual FE models with the solid187 element (see Tab. 24), a value stabilization (slowing down of the value changes) is observed for individual frequencies for models with elements side lengths ranging from 0.5 [mm] to 2 [mm]. A similar finding can be observed when analyzing the frequency errors (see Tab. 25). Within the specified element side length range, with the exception of the ω_{24} frequency, the frequency errors are negative for all other frequencies. For FE models with side lengths ranging from 4 mm to 8 mm, there are more frequencies for which the frequency error sign is positive.

Tab. 24. Values of the natural frequencies ω_{mn}[Hz] (for the different values of the length of element side of the GR1_1 wheel, solid187)

ω_{mn}		ω_{11}	ω_{21}	ω_{22}	ω_{23}	ω_{24}	ω_{31}	ω_{32}
length of element side [mm]	0.5	639.30	7343	8648.5	11353	15035	14739	17233
	0.7	639.40	7344.6	8650.4	11356	15039	14742	17237
	1	640.06	7350	8658.5	11365	15050	14756	17252
	1.5	640.79	7356	8664.8	11373	15059	14768	17264
	2	642.00	7367.8	8681	11395	15088	14799	17296
	4	648.00	7431	8783	11538	15279	15000	17493
	8	660.68	7553.5	8974	11818	15714	15342	17858

Tab. 25. Values of the frequency error ε_{mn} [%] (for the different values of the length of element side of the GR1_1 wheel, solid187)

ε_{mn}		ε_{11}	ε_{21}	ε_{22}	ε_{23}	ε_{24}	ε_{31}	ε_{32}
length of element side [mm]	0.5	-6.59	-1.57	-1.27	-0.76	0.10	-4.23	-2.09
	0.7	-6.57	-1.55	-1.25	-0.73	0.13	-4.21	-2.06
	1	-6.48	-1.48	-1.16	-0.66	0.20	-4.12	-1.98
	1.5	-6.37	-1.39	-1.09	-0.59	0.26	-4.04	-1.91
	2	-6.19	-1.24	-0.90	-0.39	0.45	-3.84	-1.73
	4	-5.32	-0.39	0.26	0.86	1.72	-2.53	-0.61
	8	-3.46	1.25	2.44	3.30	4.62	-0.31	1.47

For the FE models with the solid186 element (see Tab. 26), a stabilization of the values for individual frequencies is observed for the FE models with element side lengths ranging from 0.5 [mm] to 4 [mm]. For the FE model with an element side length up to 8 [mm], a positive value of the frequency error occurs for two frequencies. The fitting results of the FE models with the solid186 element are only slightly less favorable compared to the results in Tab. 25.

Tab. 26. Values of the frequency error ε_{mn} [%] (for the different values of the length of element side of the GR1_1 wheel, solid186)

ε_{mn}		ε_{11}	ε_{21}	ε_{22}	ε_{23}	ε_{24}	ε_{31}	ε_{32}
length of element side [mm]	0.5	-6.67	-1.64	-1.35	-0.83	0.04	-4.30	-2.17
	0.7	-6.64	-1.63	-1.35	-0.82	0.05	-4.30	-2.16
	1	-6.62	-1.63	-1.33	-0.81	0.05	-4.28	-2.15
	1.5	-6.49	-1.55	-1.27	-0.76	0.09	-4.22	-2.10
	2	-6.62	-1.61	-1.27	-0.73	0.19	-4.24	-2.03
	4	-6.16	-1.44	-1.22	-0.69	0.20	-4.17	-1.91
	8	-6.09	-0.65	-0.06	0.60	1.88	-3.57	-0.96

For FE models generated using the solid185 element (see Tab. 27), a certain stabilization of the frequency values is observed for frequency groups within the element site length range from 0.7 mm to 1.5 mm. The simulation results from the FE models within the specified element length range demonstrate a favorable match with the experimental results. A less favorable fit (frequency errors above 10%) is observed for FE models with element side of 0.5 [mm], 4 [mm], and 8 [mm].

DOI 10.2478/ama-2025-0090

Tab. 27. Values of the frequency error ε_{mn} [%] (for the different values of the length of element side of the GR1_1 wheel, solid185)

ε_{mn}		ε_{11}	ε_{21}	ε_{22}	ε_{23}	ε_{24}	ε_{31}	ε_{32}
length of element side [mm]	0.5	-6.48	-1.35	-0.10	-0.49	0.37	15.5	-1.84
	0.7	-6.30	-1.08	-0.69	-0.19	0.67	-3.76	-1.53
	1	-6.02	-0.64	-0.17	0.32	1.19	-3.35	-1.09
	1.5	-4.71	0.58	1.20	1.66	2.55	-1.86	0.28
	2	-4.60	1.45	2.57	2.95	3.87	-1.03	1.34
	4	0.82	9.37	10.8	11.5	13.2	4.22	7.49
	8	-2.92	15.4	18.4	25.9	36.9	9.90	19.6

Analyzing the obtained results (see Tabs. 25-27), it is noted that the numerical simulation results for all FE models with element side lengths ranging from 0.7 mm to 2 mm demonstrate satisfactory agreement with the experimental results. Regarding the FE models with solid186 and solid187 elements, the numerical simulation results for the remaining element side length ranges are also satisfactory. For these FE model cases (except for the errors related to the frequency ω_{11}), the frequency errors obtained are significantly below 5%, which is beneficial. For FE models with the solid185 element and with element side lengths of 0.5 mm, 4 mm, and 8 mm, for several natural frequencies, the frequency errors exceed 10%, which is very unfavorable and eliminates the usefulness of these models in the simulation process. Comparing the results in Tab. 23 with the corresponding results in Tabs. 25-27 (FE models for the case of a 1 mm element side), a better match between the simulation results and the experimental results is observed for the FE models subjected to the model tuning procedure.

In Figs. 7-13 it is show the normal modes of natural frequencies excited in the experiment and the corresponding mode shapes generated in the numerical simulation. As mentioned earlier, the analyzed wheel can be treated as a circularly symmetric plate, and shapes of the normal modes in which the nodal lines form circles and nodal diameters are expected. The displacement values of individual points generated for individual mode shapes in the numerical simulation and experiment do not correspond to the actual displacements resulting from forced vibrations. In Figs. 7-13, the areas with the expected largest relative point displacements are colored red or blue. Areas with minimal or zero relative point displacements are colored green (so-called nodal line areas). Analyzing the shapes of the obtained natural forms, it can be concluded that they are not as regular as those of a classic circularly symmetrical plate, but they are sufficiently recognizable and show mutual shape similarity. The geometry of the gear rim teeth does not significantly affect the shape of the individual normal modes. Therefore, there is no need to use the additional mode shapes similarity criterion (MAC value) [4].

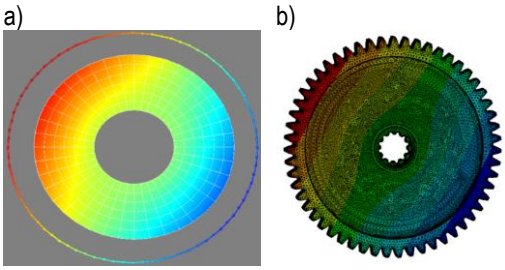

Fig. 7. Mode shapes related to frequency ω_{11}: a) experimental results, b) full FE model

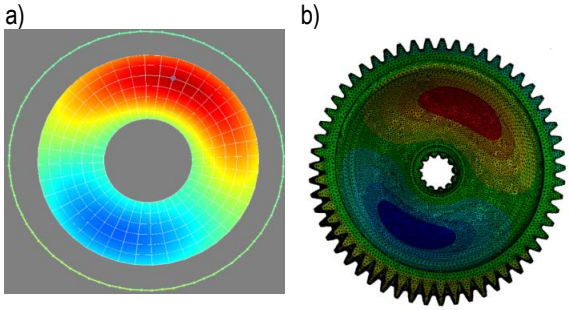

Fig. 8. Mode shapes related to frequency ω_{21}: a) experimental results, b) full FE model

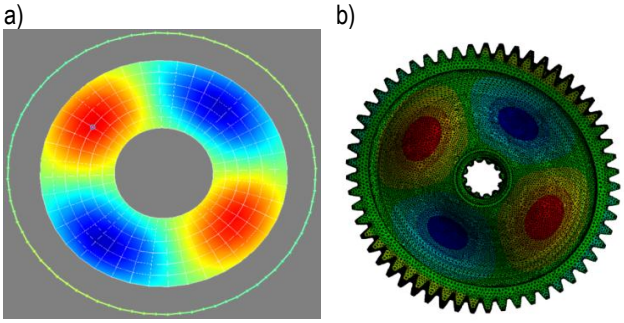

Fig. 9. Mode shapes related to frequency ω_{22}: a) experimental results, b) full FE model

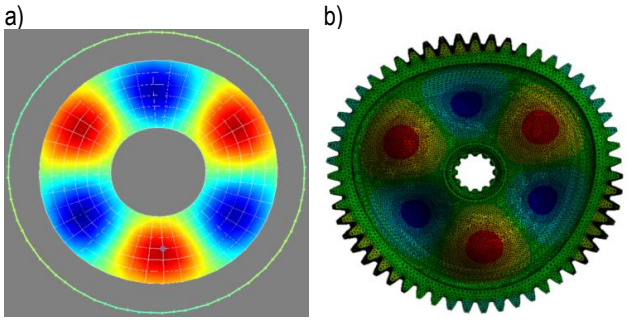

Fig. 10. Mode shapes related to frequency ω_{23}: a) experimental results, b) full FE model

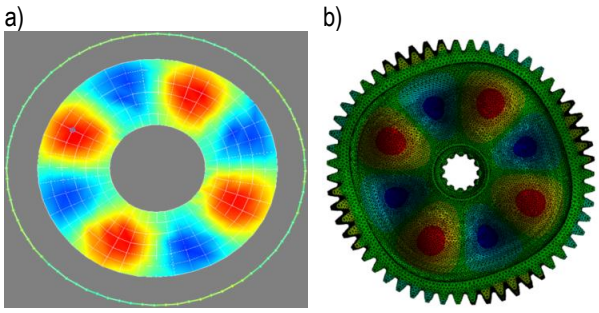

Fig. 11. Mode shapes related to frequency ω_{24}: a) experimental results, b) full FE model

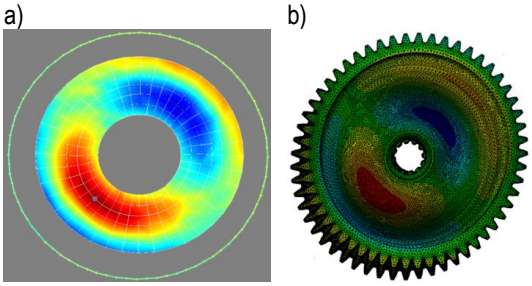

Fig. 12. Mode shapes related to frequency ω_{31}: a) experimental results, b) full FE model

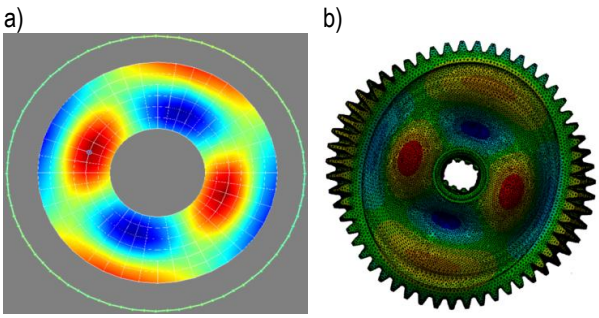

Fig. 13. Mode shapes related to frequency ω_{32}: a) experimental results, b) full FE model

6. CONCLUSIONS

The paper deals with the natural transversal vibrations of toothed wheels designed for use in aircraft power transmission systems or in the transmission of aviation engine aggregates. The analysis was lead by using wheels with straight, oblique and circular-arc teeth, as well as with a full wheel disc and a wheel disc with eccentric holes. Simplified geared rim models were proposed for each gear in the form of uniform ring made of the material with satisfactory physical properties. In the proposed simplified models were also taken into account the cyclic symmetry properties observed in the studied objects. The required numerical calculations were performed using the commercial ANSYS software. The influence of the type and size of finite elements on the quality of the obtained results was also examined. Simplified FE models of gears include a significantly smaller number of finite elements compared to the corresponding high resolution reference models.

The numerical calculations conducted using the proposed methodology were analyzed in two categories: statistical analysis of the calculation process and the quality of the proposed simplified models in terms of the adopted criterion. For statistical analysis, the following parameters were considered: relative elapsed time (WO), sum of memory used by all processes (MU), and sum of disk space used (RU).

Considering the values of the previously mentioned statistical results obtained for a computer with the technical parameters specified in the article and the ease of generating simplified models of satisfactory mesh quality, it seems reasonable to conclude that the use of the solid187 element in the FEM mesh generation process of individual models is beneficial.

In the case of testing the quality of the results generated by the proposed simplified models, the analysis results obtained from the full FE models of the considered wheels with the finite element solid187 were taken as reference data. Analyzing the obtained results, it can be seen that in all cases of the simplified FE models, the frequency error values are below 5%, which is a satisfactory result. For all the wheels in question, the fit of the results achieved from the simplified FE models with the solid187 element is relatively favorable. In computational practice [3, 4], the fitting results are considered favorable and acceptable if the frequency errors for individual natural frequencies, excluding the frequency with the lowest value, do not exceed 5%.

Considering the results from the experimental studies, it can be concluded that the results obtained for each FE model of the tested wheel are generally satisfactory. However, the best agreement with respect to the adopted criterion is demons trated by the results from the model with the solid186 element. The model with the solid187 element also demonstrates a comparable fit. Considering the signs of the frequency error (see Table 23), it can be concluded that the developed FEM models are characterized by slightly lower transversal stiffness compared to the actual tested object. Considering the analysis results regarding the effect of element size on the quality of the obtained results, it can be seen that for the wheel in question, satisfactory results can be obtained from FE models with solid185, solid186, and solid187 elements with element side lengths ranging from 0.7 mm to 2 mm. All FE models of the gear wheels analyzed in this work fall within this range. It is also beneficial to perform a procedure for tuning FE models to the experimental results. It can also be seen that satisfactory results of compliance with experimental test are generated from FE models of a wheel with solid186 and solid187 elements with element side lengths of 0.5 mm, 4 mm and 8 mm.

When developing simplified FE models with cyclic symmetry, the geometric shape of the model (including the segment angle) must first be determined. The preferred finite element is solid187 or equivalent. If possible, retain the gear rim geometry. If not, develop an equivalent gear rim model according to the procedure outlined in this paper. Next, the mesh density is determined using the model tuning procedure or, if not necessary, by numerical FEM calculations with available technical data.

The conducted analyses indicate that the effective use of simplified models and the appropriate selection of the finite element type significantly improve the advanced computational process, with a slight, and in some cases negligible, increase in the fitting errors of the proposed simplified FE models. It should be noted that the presented research fit into the contemporary trends of automation and acceleration of numerical calculations, and may be helpful to engineers dealing with the vibration analysis of gear wheels.

Nomenclature

E – Young moduli,
E_z – equivalent Young's modulus,
MAC – modal assurance criterion,
MU – sum of memory used by all processes,
N – number of segments,
RU – sum of disk space used by all processes,
WO – relative elapsed time,
k – the harmonic index,
k_L – the summation limit,
m – the number of nodal circles,
n – the number of nodal diameters,
n_K – the superscript refers to the segment number,
u – the component of physical phenomenon in segments,
$\bar{u}$ – cyclic components,
α – the angle of segment,
β – the angle of rotation of nodal lines,
ε – the frequency error,
ν – Poisson's ratio,
ρ – density,
ρ_z – equivalent density,
ω^e – the natural frequency of the reference system,
ω^f – the natural frequency comes from the numerical model,
ω_{mn} – the natural frequency of the transverse vibration.

REFERENCES

1. de Silva C. Vibration and Shock Handbook. Boca Raton: Taylor & Francis; 2005.
2. Noga S. Analytical and Numerical Problems of Systems with Circular

Symmetry Vibrations. Rzeszów: Publishing House of Rzeszow University of Technology; 2015.
3. Drago RJ, Brown FW. The analytical and experimental evaluation of resonant response in high – speed, lightweight, highly loaded gearing. Journal of Mechanical Desing. 1981;103:346-356. https://doi.org/10.1115/1.3254914
4. Friswell M, Mottershead J. Finite Element Model Updating in Structural Dynamics. Dordrecht: Kluwer Academic Publishers; 1995.
5. Rao SS. Vibration of Continuous Systems. Hoboken: Wiley; 2007.
6. Noga S, Maciejowska K, Rogalski T., Vibration analysis of an aviation engine turbine shaft shield. Aircraft Engineering and Aerospace Technology. 2021;93(9):1478-1487. https://doi.org/10.1108/AEAT-11-2020-0274
7. Davar A, Azarafza R. Free vibration analysis of functionally graded annular circular plates using classical thin plate theory based on physical neutral surface. Journal of Vibration Engineering & Technologies. 2024;12:3873-3896. https://doi.org/10.1007/s42417-023-01092-3
8. Bogacz R, Noga S. Free transverse vibration analysis of a toothed gear. Archive of Applied Mechanics. 2012;82(9):1158 – 1168. https://doi.org/10.1007/s00419-012-0608-6
9. Noga S, Markowski T. Vibration analysis of a low – power reduction gear. Strength of Materials. 2016;48(4):507-514. https://doi.org/10.1007/s11223-016-9792-x
10. Petrov EP. A method for use of cyclic symmetry properties in analysis of nonlinear multiharmonic vibrations of bladed discs. Proceedings of ASME Turbo Expo 2003. June 16 – 19. Atlanta. Georgia. USA. GT – 2003 – 38480. https://doi.org/10.1115/1.1644558
11. Naseralavi SS, Salajegheh E, Salajegheh J, Fadaee MJ. Detection of damage in cyclic structures using an eigenpair sensivity matrix. Computers & Structures. 2012; 110 -111: 43-59. https://doi.org/10.1016/j.compstruc.2012.06.003
12. Dong B. Modal Analysis of General Cyclically Symmetric Systems with Applications to Multi-Stage Structures. PhD Dissertation. Blacksburg: Virginia Polytechnic Institute and State University; 2019. http://hdl.handle.net/10919/102605
13. Noga S. Transverse vibration analysis of a compound plate with using cyclic symmetry modelling. Vibration in Physical System. 2014; 26: 211-216.
14. Noga S. Numerical and experimental analyses of vibrations of annular plates with multiple eccentric holes. Strength of Materials. 2016; 48(4): 524-532. https://doi.org/10.1007/s11223-016-9794-8
15. Gao N, Wei Z, Wang Ch, Zhu D, Wang S. Experimental and analytical studies on eliminating natural frequency splitting of an axisymmetric structure with cyclically symmetric feature groups. Journal of Sound and Vibration. 2023; 562: 117829. https://doi.org/10.1016/j.jsv.2023.117829
16. Shi X, Li Ch, Wei F. Unified approach for vibration analyses of annular sector and annular plates with general boundary conditions. Journal of Shanghai Jiaotong University (Science). 2017,22:449 – 458. https://doi.org/10.1007/s12204-017-1848-y
17. Noga S, Bogacz R, Frischmuth K. Vibration analysis of toothed gear with cyclic symmetry modelling. Vibration in Physical System. 2012; 25:299-304.
18. Noga S, Kwolek K. Free vibration analysis of aviation toothed gear with using cyclic symmetry modelling. Mechanical Overview. 2018; 11:47-51. https://doi.org/10.15199/148.2018.11.10
19. Fudali P, Jagiełowicz PE, Kalina A, Połowniak P, Sobolak M, Witkowski W. A novel method for determining the contact pattern area in gear meshing based on computer processing of pressure measurement film images. Materials. 2025;18(14): 3230 – 3272. https://doi.org/10.3390/ma18143230
20. Fudali P, Markowski T, Pacana J, Machining simulation of Novikov profile gear models for analysis and computational calculations. Materials. 2025, 18(5):1155-1170. https://doi.org/10.3390/ma18051155
21. Wang S, Xiu J, Cao S, Liu J. Analytical treatment with rigid – elastic vibration of permanent magnet motors with expanding application to cyclically symmetric power – transmission systems. ASME Journal of Vibration and Acoustics. 2014; 136(2): 021014. https://doi.org/10.1115/1.4025993
22. Kaveh A, Hamedani KB, Joudaki A, Kamalinejad M. Optimal analysis for optimal design of cyclic symmetric structures subject to frequency constraints. Structures. 2021; 33: 3122-3136. https://doi.org/10.1016/j.istruc.2021.06.054
23. Laxalde D, Lombard JP, Thouverez F. Dynamics of multistage bladed disks systems. Journal of Engineering for Gas Turbines and Power. 2007; 121:1058-1064. https://doi.org/10.1115/1.2747641
24. Voldrich J, Polach P, Lazar J, Misek T. Use of cyclic symmetry properties in vibration analysis of bladed disks with friction contacts between blades. Procedia Engineering. 2014; 96:500-509. https://doi.org/10.1016/j.proeng.2014.12.122
25. Min JB, Reddy TSR, Bakhle MA, Coroneos RM, Stefko GL, Provenza AJ, Duffy KP. Cyclic symmetry finite element forced response analysis of a distortion – tolerant fan with boundary layer ingestion. AIAA Paper 2018 – 1890. AIAA Aerospace Sciences Meeting. Kissimmee. Florida; 2018. https://doi.org/10.2514/6.2018-1890
26. Martin A, Thouverez F. Dynamic analysis and reduction of a cyclic symmetric system subjected to geometric nonlinearities. Journal of Engineering for Gas Turbines and Power. 2019;141:041027. https://doi.org/10.1115/1.4041001

The authors are grateful to EC TEST Systems Sp. z o. o. of the ENERGOCONTROL group for conducting the experimental research for the purposes of this work and for granting permission to publish these experimental data.

Stanisław Noga: https://orcid.org/0000-0003-3789-4899

Paweł Fudali: https://orcid.org/0000-0002-1976-0902